

Primary and secondary organic aerosols in 2016 summer of Beijing

Rongzhi Tang¹, Zepeng Wu¹, Xiao Li¹, Yujue Wang¹, Dongjie Shang¹, Yao Xiao¹,
Mengren Li¹, Limin Zeng¹, Zhijun Wu¹, Mattias Hallquist², Min Hu¹, Song Guo^{1,*}

*¹State Key Joint Laboratory of Environmental Simulation and Pollution Control,
College of Environmental Sciences and Engineering, Peking University, Beijing,
100871, PR China*

*²Atmospheric Science, Department of Chemistry and Molecular Biology, University
of Gothenburg, Sweden*

* Correspondence to: Song Guo, songguo@pku.edu.cn

1 **Abstract**

2 To improve the air quality, Beijing government has employed several air pollution
3 control measures since 2008 Olympics. In order to investigate the organic aerosol
4 sources after the implementation of these measures, ambient fine particulate matters
5 were collected at a regional site Changping (CP) and an urban site Peking University
6 Atmosphere Environment MonitoRing Station (PKUERS) during the “Photochemical
7 Smog in China” field Campaign in summer of 2016. A chemical mass balance (CMB)
8 modeling and the tracer yield method were used to apportion the primary and
9 secondary organic sources. Our results showed that the particle concentration
10 decreased significantly during the last a few years. The apportioned primary and
11 secondary sources explained $62.8 \pm 18.3\%$ and $80.9 \pm 27.2\%$ of the measured OC at
12 CP and PKUERS, respectively. Vehicular emissions served as the dominant sources.
13 Except gasoline engine emission, the contributions of all the other primary sources
14 decreased. Besides, the anthropogenic SOC, i.e. toluene SOC, also decreased,
15 implying that deducting primary emission can reduce anthropogenic SOA. Different
16 from the SOA from other regions in the world, where biogenic SOA was dominant,
17 anthropogenic SOA was the major contributor to SOA, implying that deducting
18 anthropogenic VOCs emissions is an efficient way to reduce SOA in Beijing. Back
19 trajectory cluster analysis results showed that high mass concentrations of OC were
20 observed when the air mass was from south. However, the contributions of different
21 primary organic sources were similar, suggesting the regional particle pollution. The
22 ozone concentration and temperature correlated well with the SOA concentration.
23 Different correlations between day and night samples suggested the different SOA
24 formation pathways. Significant enhancement of SOA with increasing particle water
25 content and acidity were observed in our study, suggesting the aqueous phase
26 acid-catalyzed reactions may be the important SOA formation mechanism in summer
27 of Beijing.

28 **1. Introduction**

29 Beijing is the capital and a major metropolis of China. With the rapid economic
30 growth and urbanization, Beijing is experiencing serious air pollution problems, and
31 became one of the hotspots of PM_{2.5} (particulate matters with size smaller than 2.5 μ m)
32 pollution in the world (Guo et al., 2014a; Xiang et al., 2017; Tian et al., 2016). Due to
33 the frequent haze events in Beijing, Beijing government has taken a series of control
34 measures in recent years, especially after 2008 Olympics, which may greatly
35 influence the primary and secondary particle sources. Therefore, elucidating the
36 current contributions of primary particle sources as well as secondary particle sources
37 is of vital importance. It is also important to compare with the previous results to
38 evaluate the effectiveness of the control measures and shed light on the influence of
39 the primary source emission control on the secondary aerosol formation.

40 Several studies regarding to the source apportionment of fine particles in Beijing have
41 been conducted using multifarious methods during the last few years (Yu et al., 2013;
42 Gao et al., 2014; Zheng et al., 2016b; Tan et al., 2014; Wang et al., 2009; Guo et al.,
43 2013). Receptor model is a commonly used method to apportion the particle sources
44 (Zhang et al., 2017; Zhou et al., 2017; Zhang et al., 2013; Song et al., 2006; Zheng et
45 al., 2005). Elemental tracers were previously used to apportion particulate matter
46 sources (Yu et al., 2013; Gao et al., 2014; Zheng et al., 2016b). However, elemental
47 tracer-based method was unable to distinguish sources that mostly emit organic
48 compounds instead of specific elements such as diesel/gasoline engines. Among all
49 the apportionment methods, chemical mass balance (CMB) model was one of the
50 most commonly used methods to apportion the primary organic sources of fine
51 particulate matter (Zhang et al., 2017; Hu et al., 2015; Schauer et al., 1996). Organic
52 tracers have been successfully used in several studies which aimed to quantify the
53 main sources of Beijing (Liu et al., 2016; Guo et al., 2013; Wang et al., 2009). Wang
54 et al. assessed the source contributions of carbonaceous aerosol during 2005 to 2007

55 (Wang et al., 2009). Guo et al. (Guo et al., 2013) and Liu et al. (Liu et al., 2016)
56 apportioned the organic aerosol sources using CMB model in summer of 2008 and a
57 severe haze event in winter of 2013. Both studies found that vehicle emission and coal
58 combustion were the dominant primary sources of fine organic particles. Tracer-yield
59 method has been considered as a useful tool to semi-quantify SOA derived from
60 specific VOCs precursors (Guo et al., 2012; Zhu et al., 2017; Zhu et al., 2016; Tao et
61 al., 2017; Hu et al., 2008). However, only a few studies have estimated secondary
62 organic aerosol in Beijing. Yang et al. (Yang et al., 2016) estimated the biogenic SOC
63 to OC during CAREBEIJING-2007 field campaign, and found that the **biogenic** SOC
64 accounted for 3.1% of the measured OC. Guo et al. (Guo et al., 2012) illustrated the
65 SOA contributions in 2008, and found that secondary organic carbon could contribute
66 a great portion ($32.5 \pm 15.9\%$) to measured organic carbon at the urban site. Ding et al.
67 (Ding et al., 2014) used the tracer-yield method to investigate the SOA loading on a
68 national scale and found that SOA, especially anthropogenic SOA played great role in
69 major city clusters of China.

70 In this study, we quantified 144 kinds of particulate organic species, including
71 primary and secondary organic tracers, at a regional site and an urban site of Beijing.
72 A CMB modeling and the tracer yield method were used to apportion the primary and
73 secondary sources of the organic aerosols in the 2016 summer of Beijing. The results
74 were compared with the previous studies to evaluate the effectiveness of control
75 measures on primary as well as secondary organic aerosols. Moreover, source
76 apportionment results from different air mass origins according to the back trajectory
77 clustering analysis were shown to investigate the influences of air mass from different
78 directions on the fine organic particle sources. Influencing factors of SOA formation,
79 i.e. temperature, oxidant concentration, aerosol water content, as well as particle
80 acidity were also discussed in this study to improve our understanding of SOA
81 formation under polluted environment.

82 2. Experimental

83 2.1 Sampling and Chemical Analysis

84 The measurements were conducted simultaneously at an urban site Peking University
85 Atmosphere Environment MonitoRing Station (PKUERS, 39°59'21" N, 116°18'25" E)
86 and a regional site Changping (CP, 40°8'24"N, 116°6'36" E) 40km north of PKUERS
87 site during "Photochemical Smog in China" campaign, from May 16th to June 5th,
88 2016 (see Fig. S1) (Hallquist et al., 2016). The PKUERS site is set on the roof at an
89 academic building on the campus of Peking University in the northwest of Beijing.
90 CP site is located on the fourth floor of a building on the Peking University
91 Changping campus of Changping.

92 Four-channel samplers (TH-16A, Tianhong, China) consisting of three quartz filter
93 channel and one Teflon filter channel, were employed to collect 12-h aerosol samples
94 at PKUERS and CP, respectively. The sampling flow rate was 16.7 L min⁻¹. Teflon
95 filters were weighed by a microbalance (Toledo AX105DR, USA) after a 24 h balance
96 in an environmental controlled room (temperature 20 ± 1°C, relative humidity 40 ±
97 3%) for gravimetric analysis. Teflon-based samples were extracted by deionized water
98 to measure water-soluble inorganic compounds (WSICs), namely Na⁺, NH₄⁺, K⁺,
99 Mg²⁺, Ca²⁺, NO₃⁻, SO₄²⁻ and Cl⁻ by DIONEX ICS-2500 and ICS-2000
100 ion-chromatograph. One punch (1.45 cm²) of quartz-based sample was then cut off to
101 analyze the EC and OC via thermal-optical method using Sunset Laboratory-based
102 instrument (NIOSH protocol, TOT). The other two quartz filters were then extracted
103 and analyzed for chemical composition and particulate organic matters. Some daytime
104 and nighttime samples were combined to ensure the detection of most organic
105 compounds. To better understand the chemical speciation, daytime samples were
106 separated from nighttime samples.

107 Authentic standards were used to identify and quantify the organic compounds. The
108 analytical methods used in this study referred to the previous work (Song et al., 2014).

109 Briefly, the samples were first spiked with a mixture of internal standard, including
110 ketopinic acid (KPA), 20 kinds of deuterated compounds, and one carbon isotope
111 ¹³C-substituted compound. The quartz filters were then ultrasonically extracted with
112 methanol: dichloromethane (v:v=1:3) solvent in water bath (temperature < 30 °C) for
113 3 times. Each time was 20 min. The extracts were filtered, and then concentrated
114 using a rotary vacuum evaporator. An ultra-pure nitrogen flow was used to further
115 concentrate the extracts into 0.5-1 ml. Each extracted solution was divided into two
116 portions, one of which added BSTFA (BSTFA/TMCS = 99:1, Supelco) to convert
117 polar organic compounds into trimethylsilylated derivatives. Afterwards, the
118 derivatized and the untreated samples were analyzed by an Agilent 6890 GC-MS
119 System (MSD GC-5973N) equipped with an Agilent DB-5MS GC column (30 m ×
120 0.25 mm × 0.5 μm).

121 **2.2 Source Apportionment**

122 A chemical mass balance modelling developed by the U.S. Environmental Protection
123 Agency (EPA CMB version 8.2) was applied to determine the apportion of the
124 primary contribution of OC (Schauer et al., 1996). This receptor model solved a set of
125 linear equations using ambient concentrations and chemical source profiles. CMB
126 approach depends strongly on the representativeness of the source profile. In this
127 study, five primary source profiles including vegetative detritus (Rogge et al., 1993),
128 coal combustion (Zheng et al., 2005), gasoline engines (Lough et al., 2007), diesel
129 engines (Lough et al., 2007) as well as biomass burning (Sheesley et al., 2007) were
130 input into the model. Fitting species including EC, n-alkanes, levoglucosan,
131 17β(H)-21α(H)-norhopane, 17α(H)-21β(H)-hopane, benzo(b)fluoranthene,
132 benzo(k)fluoranthene, benzo(e)pyrene, benzo(ghi)perylene, indeno(1,2,3-cd)pyrene.
133 The criteria for acceptable fitting results included the square regression coefficient of
134 the regression equation $R^2 > 0.85$ as well as the sum of square residual Chi-square
135 value $\chi^2 < 4$.

136 The tracer yield method was used to estimate the contributions of biogenic and
137 anthropogenic secondary organic aerosols using fixed tracers to SOC ratio (f_{SOC})
138 based on laboratory experiments, which was 0.155 ± 0.039 for isoprene, 0.231 ± 0.111
139 for α -pinene, 0.0230 ± 0.0046 for β -caryophyllene and 0.0079 ± 0.0026 for toluene
140 (Kleindienst et al., 2007). The mass fraction depends on the degree of oxidation.
141 Besides, the uncertainty also depends on the selection of molecular tracers and the
142 simplified procedures by using single-valued mass fractions (Yttri et al., 2011; El
143 Haddad et al., 2011; Song et al., 2014; Guo et al., 2014b; Guo et al., 2014c). Previous
144 studies showed that SOA estimated by the tracer-yield method and POA apportioned
145 by CMB model could fully account for the OA in atmospheric atmosphere
146 (Lewandowski et al., 2008; Kleindienst et al., 2010). Besides, researchers found that
147 the total estimated SOC derived from tracer-yield method was in accordance with the
148 that stemmed from EC-tracer method during summer (Ding et al., 2012; Kleindienst
149 et al., 2010; Turpin and Huntzicker, 1995). Comparable results were also found
150 between tracer-yield method and positive matrix factorization model (Hu et al., 2010;
151 Zhang et al., 2009). All these results firmly demonstrated that the tracer-yield method
152 is a valuable and convincing method to estimate the SOA contributions (X. Ding et al.,
153 2014).

154 Estimations based on boundary values were generally acknowledged to have the
155 largest source of uncertainties in the models, so those results could be used to
156 determine the possible limit of the estimations. Also, Kleindienst et al. carried out a
157 boundary analysis using the data from North California to measure the range of
158 estimated SOA contributions. Results revealed that the possible contributions of
159 isoprene, α -pinene, β -caryophyllene and toluene were within the scope of 70-130%,
160 50-220%, 70-120% and 60-160%, respectively. The above results were supposed to
161 be in the acceptable range for PM_{2.5} source apportionment. Besides, the standard
162 deviations of the tracer-to-SOC ratios were suitable as a source profile uncertainty
163 (Kleindienst et al., 2007). Despite the uncertainties above, tracer-yield represented a

164 unique approach to estimate the SOA contributions using individual hydrocarbon
165 precursors up to now.

166 3. Gaseous pollutants and particle chemical composition

167 3.1 Gaseous pollutants and meteorological conditions of the observation period

168 Mixing ratios of gaseous pollutants and meteorological conditions during the
169 observation period were shown in Fig. S2 and Table S1. Compared with the results in
170 summer of 2010 (Zheng et al., 2016a), the gaseous mixing ratios SO₂ and CO were
171 lower than before owing to the desulfurization efforts made by the government.
172 Higher concentrations of NO and NO₂ were caused by the increasing number of
173 vehicles. The increment of ozone indicated the importance of secondary pollution.
174 Clearly, ozone concentration at CP was higher than that of PKUERS while other
175 pollutants were lower.

176 During the campaign, the average wind speed was low, showing average values of 2.3
177 ± 1.4 m/s and 2.4 ± 1.5 m/s at CP and PKUERS, respectively. The diurnal variations
178 of wind directions and speeds are exhibited in Fig. S2. The prevailing wind was from
179 south, with higher wind speed during the daytime.

180 To explore the influence of the air masses from different directions on fine particle
181 loading and sources, back trajectory analysis was performed using National Oceanic
182 and Atmospheric Administration (NOAA) Hybrid Single Particle Lagrangian
183 Integrated Trajectory (HYSPLIT) model. We calculated 36 h air mass back
184 trajectories arriving at two sampling site during the observation period using the
185 HYSPLIT-4 model with a 1°×1° latitude-longitude grid and the final meteorological
186 database. The model was run with the starting time of 0:00, 4:00, 8:00, 12:00, 16:00,
187 and 20:00 UTC). The arrival level was set at 200 m above ground level. The method
188 used in trajectory clustering was based on GIS-based software TrajStat
189 (<http://www.meteothinker.com/TrajStatProduct.aspx>). 36-h back trajectories starting at
190 200 m above ground level in CP and PKUERS were calculated every 4 hours during

191 the entire campaign and then clustered according to their similarity in spatial
192 distribution using the HYSPLIT4 software. Three-cluster solution was adopted as
193 shown in Fig. S3. The three clusters were defined as Far North West (Cluster 1, Far
194 NW), Near West North (Cluster2, Near WN), and South (Cluster 3). South cluster was
195 found to be the most frequent one, accounting for 52% at CP and 64% at PKUERS.
196 Clusters Far NW and Near NW accounted for 17% and 31%, 17% and 19% at CP and
197 PKUERS, respectively.

198 **3.2 Overview of PM_{2.5} chemical composition**

199 In this study, daily PM_{2.5} concentrations fluctuated dramatically from 6.7 $\mu\text{g m}^{-3}$ to
200 80.3 $\mu\text{g m}^{-3}$ at CP, and from 9.6 to 82.5 $\mu\text{g m}^{-3}$ at PKUERS, respectively. A paired
201 t-test was used to compare the mass concentrations at two sites. The results indicate
202 that the mass concentrations showed statistically non-significant difference,
203 suggesting the regional particle pollution in Beijing. PM_{2.5} mass concentrations during
204 the summer of 2008 to 2016 in Beijing are summarized in Table 1. Guo et al. (Guo et
205 al., 2013) reported the average PM_{2.5} concentrations during the summers of 2000 to
206 2008, which showed distinct decreasing tendency during 2000-2006 and then slightly
207 increased in 2007 due to unfavorable meteorological conditions. To better understand
208 the variation tendency of the PM_{2.5} in the summer of Beijing, we compared the fine
209 particle matter data since 2008. Compared with 2008, the PM_{2.5} concentrations
210 decreased from $92.3 \pm 44.7 \mu\text{g m}^{-3}$ to $88.2 \mu\text{g m}^{-3}$ in 2009 and $62.7 \mu\text{g m}^{-3}$ in 2010.
211 The mass concentration continued falling to $45.5 \mu\text{g m}^{-3}$ in 2016. This decreasing is
212 attributed to the drastic emission control measures implemented by the Beijing
213 government since 2012. In spite of the prominent decrease of the PM_{2.5} mass
214 concentrations, the aerosol loading in Beijing was still much higher than that in
215 developed countries (Tai et al., 2010; Barmpadimos et al., 2012; Park and Cho, 2011).
216 Fig. S4 showed the chemical composition of PM_{2.5}. In general, organic particulate
217 matters (OM, OC*1.6) and sulfate were the two dominant components, accounting for

218 more than 50% of the PM_{2.5} mass concentration during the field campaign. The
219 average concentration of total WSICs for CP was $17.4 \pm 11.5 \mu\text{g m}^{-3}$, higher than that
220 of PKUERS ($12.2 \pm 8.5 \mu\text{g m}^{-3}$). Among the WSICs, secondary inorganic ions (sulfate,
221 nitrate, and ammonium) were the most abundant compounds, indicating secondary
222 particles played great roles in the summer of Beijing. The higher sulfate proportion
223 could be explained by the increased photochemical conversion of sulfur dioxide to
224 sulfate aerosol (Xiang et al., 2017). Relevant data of main WSICs (sulfate, nitrate and
225 ammonia) during 2008 to 2016 were also included in table 1 to better elucidate the
226 drastic decrease of fine particulate matter in recent years. Results showed that the
227 daily average concentration of WSICs decreased from 2008 to 2016, with sulfate
228 decreased from $35.6 \mu\text{g/m}^3$ to $4.7 \mu\text{g/m}^3$, nitrate decreased from $7.9 \mu\text{g/m}^3$ to 2.4
229 $\mu\text{g/m}^3$, ammonia decreased from $15.2 \mu\text{g/m}^3$ to $3.5 \mu\text{g/m}^3$. The significant decrease of
230 WSICs confirmed the effectiveness of the control measures taken by the government.

231 Carbonaceous aerosols, i.e. organic carbon (OC) and elemental carbon (EC) were also
232 great contributors to PM_{2.5} concentrations. Higher proportion of OC and EC at
233 PKUERS demonstrated severe carbonaceous pollution in urban Beijing, which might
234 have close correlation with the higher traffic flow, coal/wood combustion by residents
235 and industrial emissions (Wang et al., 2006; Dan et al., 2004; Cao et al., 2004).
236 Comparison of the OC, EC concentrations from 2008 to 2016 were also listed in Table
237 1. Unlike PM_{2.5}, OC concentration at PKUERS showed a higher OC concentration
238 ($11.0 \pm 3.7 \mu\text{g m}^{-3}$) compared with that in 2008 ($9.2 \pm 3.3 \mu\text{g m}^{-3}$), suggesting organic
239 aerosol pollution becomes more and more important. EC concentration decreased
240 dramatically to $0.7 \pm 0.5 \mu\text{g m}^{-3}$ at CP and $1.8 \pm 1.0 \mu\text{g m}^{-3}$ at PKUERS, which
241 showed the lowest value since 2000. This could be attributed to the implementation of
242 air pollution prevention and control action plan enacted by the state council since
243 2013. Therefore, we could draw a conclusion that the drastic decrease of fine
244 particulate matter in Beijing was mainly due to the well-controlled EC and WSICs,
245 with negligible contribution of OC.

246 To evaluate the influences of the air masses from different directions on the PM_{2.5}
247 loadings during the campaign, three categories were divided according to the back
248 trajectory clustering analysis (See Fig. S5). In general, cluster south represented the
249 most polluted air mass origin followed by clusters Near WN and Far NW, which was
250 in accordance with previous studies demonstrating severe aerosol pollution in
251 southerly air flow in summer of Beijing (Huang et al., 2010; Sun et al., 2010).

252 **3.3 Concentration of particulate organic species from different air mass origins**

253 The organic species (except secondary organic tracers) were divided into 12
254 categories. Their concentrations in different directions according to the back trajectory
255 clustering were shown in Fig. S6. Detailed information for each class at the two sites
256 could be found in the supplementary material (Fig. S7). Cluster south showed higher
257 particulate organic matter concentration, followed by cluster near WN and far NW,
258 indicating more severe aerosol pollution from the south. Our result consists with the
259 previous studies that more pollution emissions are from the south area of Beijing than
260 those from the north (Wu et al., 2011; Zhang et al., 2009).

261 **For all the species, the histogram showed the daily average concentrations with error**
262 **bars representing one standard deviation.** Dicarboxylic acid was the most abundant
263 species among all the components, demonstrating the great contribution of the
264 secondary formation to the organic aerosols in the summer of Beijing (Guo et al.,
265 2010). A series of n-alkanes ranging from C₁₂ to C₃₆ were analyzed. Their
266 distribution during the observation period was shown in Fig. S7 (a). The
267 maximum-alkane concentration species (C_{max}) were C₂₇ and C₂₉. The odd carbon
268 preference was an indicative of biogenic sources (vegetative matters and biomass
269 burning) (Huang et al., 2006; Rogge et al., 1993). In this study, total PAHs were much
270 lower than previous studies in summer of Beijing, suggesting the effectiveness of the
271 control strategies since 2013 (Wang et al., 2009). According to Fig. S7 (c), five ring
272 PAHs were dominant species among all the species, followed by four-ring and

273 six-ring PAHs. In total, four to six ring PAHs had higher abundancy, accounting for
274 more than 60% of the total PAHs. The result was much similar with previous studies
275 that the distribution of PAHs was impacted by the volatility of PAHs and the
276 temperature (Wang et al., 2009; Guo et al., 2013). Saccharide was considered to
277 originate from biomass burning (Simoneit et al., 1999). In this study, we quantified
278 three sugar compounds including levoglucosan, manosan and galactosan, in which
279 levoglucosan was considered as a good tracer for biomass burning. The average daily
280 mass concentration of levoglucosan at CP and PKUERS were $53.03 \pm 39.26 \text{ ng m}^{-3}$
281 and $59.87 \pm 38.93 \text{ ng m}^{-3}$, respectively. It's worth mentioning that the levoglucosan
282 concentration was the lowest in recent years (Cheng et al., 2013; Guo et al., 2013).
283 Hopanes have been considered as markers for oil combustion (Lambe et al., 2009),
284 vehicles (i.e. gasoline-powered and diesel-powered engine) (Cass, 1998; Lough et al.,
285 2007) and coal combustion (Oros and Simoneit, 2000). Nevertheless, contributions of
286 coal combustion to hopanes were much less than that of vehicle exhaustion.
287 Concentrations of quantified hopanes including $17\alpha(\text{H})$ -22,29,30-trishopane,
288 $17\beta(\text{H})$ -21 $\alpha(\text{H})$ -norhopane, and $17\alpha(\text{H})$ -21 $\beta(\text{H})$ -hopane of CP and PKUERS are
289 shown in Fig. S7(d). The total average concentrations of hopanes were $3.05 \pm 1.53 \text{ ng}$
290 m^{-3} for CP and $3.90 \pm 2.06 \text{ ng m}^{-3}$ for PKUERS. The **daily averaged** hopanes
291 concentrations at urban site PKUERS were much higher than that of CP, which could
292 probably explained by the heavier vehicle emissions in the urban area. The
293 concentrations of primary organic tracers used in CMB model were listed in Table S2.

294 **3.4 Biogenic and anthropogenic SOA tracers**

295 Table S3 compared the SOA tracers measured in this work with those in other regions
296 in the world as well as that observed in Beijing 2008. The sites for comparison
297 include an urban background site at Indian Institute of Technology Bombay, Mumbai,
298 India (IITB) (Fu et al., 2016), an outflow region of Asian aerosols and precursors
299 Cape Hedo, Okinawa, Japan (CH) (Zhu et al., 2016), a residential site at Yuen Long,
300 Hong Kong (YL) (Hu et al., 2008), three industrial sites at Cleveland Ohio (CL, data

301 was averaged among the three sites), a suburban site in the Research Triangle Park
302 North California (RTP). The detailed information about these sites were summarized
303 in the supplementary material.

304 Three isoprene-SOA tracers i.e. two 2-methyltetrols (2-methylthreitol and
305 2-methylerythritol) and 2-methylglyceric acid were detected. The summed
306 concentration of the isoprene-SOA tracers ranged from 3.7 to 62.3 ng m⁻³ at CP and
307 8.6 to 46.5 ng m⁻³ at PKUERS. The concentration was higher than that of IITB and
308 CH. Compared with the isoprene-SOA tracers in 2008, the concentrations in 2016
309 were lower.

310 Nine α -pinene tracers were identified. The sum of the tracers ranged from 20.9 to
311 282.3 ng m⁻³ at CP and 50.0 to 161.4 ng m⁻³ at PKUERS, which had similar
312 distribution pattern with that measured in 2008 Beijing and YL. The total α -pinene
313 tracer concentrations were lower than those in 2008, while still much higher than the
314 concentrations in other regions of the world.

315 β -caryophyllinic acid is one of the oxidation products of β -caryophyllene which is
316 considered as a tracer for β -caryophyllene SOA. In this study, β -caryophyllinic acid
317 concentrations ranged from 1.4 to 16.7 ng m⁻³ at CP, and 0.9 to 12.0 ng m⁻³ at
318 PKUERS, with average daily average concentrations of 6.1 ± 3.5 ng m⁻³ and 6.0 ± 2.8
319 ng m⁻³ for CP and PKUERS, respectively. The values were lower than those at YL and
320 RPT, higher than that measured at Yufa and PKUERS in 2008.

321 2,3-Dihydroxy-4-oxopentanoic acid is deemed as a tracer for toluene SOA. Our
322 results showed that the 2,3-Dihydroxy-4-oxopentanoic acid concentration was $9.7 \pm$
323 7.3 ng m⁻³ at CP and 11.0 ± 3.7 ng m⁻³ at PKUERS. Compared with other regions of
324 the world, the concentrations of 2,3-Dihydroxy-4-oxopentanoic acid was much higher,
325 implying higher contributions of anthropogenic sources at Beijing. However, **the**
326 **2,3-dihydroxy-4-oxopentanoic acid** concentrations in CP were lower than that of
327 PKUERS.

328 **4. Primary sources and secondary formation of organic aerosols**

329 **4.1 Contributions of primary and secondary organic aerosols**

330 A CMB model and the tracer-yield method were used to quantify the contributions of
331 primary and secondary sources to the ambient organic carbon (See Fig. 1). On
332 average, the primary sources accounted for $42.6 \pm 15.4\%$ and $50.4 \pm 19.1\%$ of the
333 measured OC at CP and PKUERS, respectively. The vehicle emissions were the
334 dominant primary sources, with the contributions of $28.8 \pm 14.8\%$ and $37.6 \pm 19.3\%$
335 at PKUERS and CP, respectively, implying the urgency to control vehicular
336 exhaustion in urban areas. Despite of the lower contribution of the gasoline exhaust at
337 PKUERS, the mass concentration of the gasoline exhaust was higher compared with
338 that of CP given the higher OC loading at PKUERS. The contributions of biomass
339 burning were $3.9 \pm 2.6\%$ and $5.0 \pm 2.2\%$ at CP and PKUERS, respectively, showing
340 the higher concentrations at night. The drastic change of the biomass burning
341 contribution in CP at night was due to occasional burning activities at night. Coal
342 combustion contributed $5.8 \pm 5.5\%$ and $4.6 \pm 2.6\%$ of the measured OC at CP and
343 PKUERS. The higher contribution at CP was due to more burning activities in the
344 suburban areas.

345 The secondary organic sources accounted for $20.2 \pm 6.7\%$ of the organic carbon at CP,
346 with $1.6 \pm 0.4\%$ from isoprene, $4.4 \pm 1.5\%$ from α -pinene, $2.7 \pm 1.0\%$ from
347 β -caryophyllene and $12.5 \pm 3.4\%$ from toluene. As for PKUERS, the secondary
348 organic sources took up $30.5 \pm 12.0\%$ of the measured OC, in which isoprene was
349 responsible for $2.3 \pm 0.9\%$, α -pinene for $5.6 \pm 1.9\%$, β -caryophyllene for $3.6 \pm 2.6\%$
350 and toluene for $19.0 \pm 8.2\%$. Haque et al. (Haque et al., 2016) used tracer-based
351 method to apportion the organic carbon and results showed that the biogenic SOC was
352 responsible for 21.3% of the total OC with isoprene SOC contributing 17.4%,
353 α/β -pinene SOC contributing 2.5% and β -caryophyllene SOC contributing 1.4% in the
354 summer of Alaska, implying the significant contributions of the biogenic SOA to the

355 loading of the organic aerosol. Our results exhibited that the biogenic SOA
356 concentration was comparable or even high than that at some forest sites in other
357 places of the world (Miyazaki et al., 2012; Stone et al., 2012; Claeys et al., 2004;
358 Kourtchev et al., 2008). The SOA formation mechanism is complicated. A possible
359 reason is the high oxidation capacity in China. Higher oxidation capacity in China
360 may fasten the chemical lifetime of reactive gases and accelerate the aerosol aging
361 process which leads to an increase in biogenic SOA (Ghirardo et al., 2016). Another
362 possible reason derived from the complicated emissions of anthropogenic VOCs
363 which can lead to an enhancement of secondary organic aerosol formation from
364 biogenic precursors (Hoyle et al., 2011). We also compare the isoprene concentration
365 with the forest site according to some literatures. Wang et al. (Wang et al., 2010)
366 discovered that the mean isoprene concentration was 0.24 ppbv at PKUERS in June
367 2008. Lappalainen et al. (Lappalainen et al., 2009) measured the isoprene
368 concentration of the boreal forest in Hyytiala and found that the mean concentration
369 of isoprene was 0.15 ppbv. This comparable, or even higher concentration of isoprene
370 may be due to different sources of biogenic VOCs. More work is still needed to
371 investigate the SOA formation mechanism under Air Pollution Complex in China.

372 Stone et al. (Stone et al., 2009) discovered that primary and secondary sources
373 accounted for $83 \pm 8\%$ of the measured organic carbon, with primary sources
374 accounted for $37 \pm 2\%$ and SOC contributed for $46 \pm 6\%$ with $16 \pm 2\%$ from biogenic
375 gas-phase precursors and $30 \pm 4\%$ from toluene using CMB model and tracer-based
376 method at Cleveland with heavy industries, implying that anthropogenic sources
377 played great roles in the formation of SOA. Our results showed a similar with the
378 results published by Stone et al., where anthropogenic sources i.e. toluene derived
379 SOC dominated the apportioned SOC. Our research revealed an important point that
380 controlling SOA seems feasible in the developing countries like China. It is difficult
381 to control SOA in developed countries, since biogenic SOA are dominant. However,
382 deducting anthropogenic precursors may be an efficient way to reduce the SOA

383 pollution where anthropogenic SOA is dominant. On average, $62.8 \pm 18.3\%$ and 80.9
384 $\pm 27.2\%$ of the measured OC were apportioned at CP and PKUERS, respectively.
385 About $36.3 \pm 18.1\%$ and $29.3 \pm 15.6\%$ of the OC sources remained unknown, which
386 were probably composed of uncharacterized primary or secondary sources. Further
387 research is needed to explain the unapportioned sources of OC.

388 Due to the drastic emission control measures taken by the Beijing government, the
389 primary and secondary sources in Beijing may change greatly. Fig. 2 displayed the
390 comparison of the sources between 2008 and 2016 at the same site PKUERS. We
391 compared the average contributions by percentage rather than the mass concentration.
392 In general, primary sources contributed $50.4 \pm 19.1\%$ of the measured OC in 2016,
393 closely correlated to the increasing contribution of vehicular emissions. Gasoline
394 engines accounted for 18% of the measured OC, showing an enhancement of 80%
395 with respect to 2008. This might be related to the rising number of the vehicles in
396 Beijing. In comparison, diesel exhaust decreased by 12.5% due to the strict control
397 measures made by the government. A 28.5% and 20% reduction of coal combustion
398 and biomass burning could also be found due to the drastic measures made by the
399 government. Compared with 2008, contributions of secondary organic aerosol
400 decreased by 29.4%, in which biogenic SOC served as the biggest contributor to this
401 decreasing. The formation of biogenic SOA is complicated. Several factors can affect
402 biogenic SOC formation, among which the precursor concentration is one of the
403 crucial factors. Biogenic VOCs, i.e. isoprene, α -pinene etc. are predominantly emitted
404 from plant foliage in a constitutive manner. The emission rate of biogenic VOCs
405 depends on various factors, e.g. radiation, temperature, humidity, meteorological
406 conditions and seasonality (Ghirardo et al., 2016). Two or more of them will act
407 synergistically to have an effect on the concentration of isoprene SOC. Besides, the
408 changes of the vegetation in certain area may also play a part in the change of the
409 SOC concentration. Considering its comprehensive synergistic effect, it's difficult to
410 determine the main reason responsible for the isoprene SOC decrease.

411 However, the contribution of toluene SOC was the highest among the apportioned
412 SOC, which was different from the results of the most developed countries in the
413 world. Compared with previous studies, except β -caryophyllene SOC, vegetative
414 detritus and gasoline exhausts, the contributions of all other sources decreased, e.g.
415 isoprene SOC, α -pinene SOC, toluene SOC, biomass burning, diesel exhaust, and coal
416 combustion. However, the increases in β -caryophyllene SOC, vegetative detritus
417 and gasoline exhausts could not compensate for the decreases of other sources. This
418 can be attributed to the larger portion of uncharacterized sources compared with 2008.
419 The uncharacterized sources may mainly contain cooking emissions, mineral and road
420 dust, industrial pollution as well as other uncharacterized secondary sources (Tian et
421 al., 2016; Liu et al., 2016). In summary, the contributions of most POA decreased in
422 recent years, except for gasoline exhaust, indicating more efforts should be made to
423 control the gasoline emission. The apportioned SOC was also decreased with toluene
424 SOC served as the dominant source. Our results revealed that deducting
425 anthropogenic precursors may be an efficient way to control SOA pollution in China.

426 **4.2 Organic aerosol sources from different air mass origins**

427 The regional sources and transport of air pollutants exert profound impacts on air
428 quality of Beijing. To better understand the regional impacts on the primary and
429 secondary aerosol sources of Beijing, source apportionment results when air mass
430 from different origins were shown in Fig. 3. Vehicular emissions i.e. gasoline and
431 diesel exhaust showed identical contributions from different air mass origins (31.0%
432 from south vs 31.3% from Near WN vs 31.7% from Far NW) at PKUERS,
433 demonstrating the vehicular pollution could mostly be attributed to the vehicular
434 emission at the local site. However, the contribution of vehicular emission at CP
435 showed significant difference from different air mass origins, with lowest contribution
436 when air mass was from far northwest. This might be explained by regional transport
437 from different directions. Comparable contributions of coal combustion and biomass
438 burning were found at CP and PKUERS from different air mass origins, implying the

439 regional pollution in Beijing. Similarly, biogenic SOC showed similar contributions
440 from different air mass origins both at the regional site and the urban site. From all the
441 directions, the toluene SOC (anthropogenic source) was the largest contributor to
442 apportioned SOC, with higher concentrations at the urban site PKUERS. On the
443 whole, most of the sources showed comparable contribution from different air mass
444 origins, implying the pollution in Beijing was regional.

445 **4.3 Influencing factors for secondary organic aerosol formation in the summer of** 446 **Beijing**

447 Laboratory experiments have revealed that several factors can influence the SOA
448 formation, e.g. oxidants (OH radical, ozone etc.), temperature, humidity, particle
449 water content and acidity. We found that the correlations between SOC and
450 ozone/temperature are different for daytime and nighttime samples. However, it's not
451 significant for water content and hydrogen ions concentration. Therefore, we separate
452 the data between day and night between SOC and ozone/temperature, and use entire
453 data for the analysis of particle water and acidity. In this work, the relationships
454 between estimated SOA and these factors were investigated to better understand the
455 SOA formation in Beijing.

456 **SOA formation from ozonolysis**

457 Ozone is considered as an important oxidant for SOA formation. Fig. 4 (a)(b) showed
458 the correlation with ozone mixing ratio and SOC. It is clear that SOC increased
459 significantly with the increasing of ozone mixing ratio, which is consistent with
460 previous studies in Beijing (Guo et al. 2012). Different correlations were found
461 between day and night samples, with better correlation for the daytime samples at
462 both sites, implying SOA may have other formation mechanism at night other than
463 ozonolysis. At CP, the growth rate of SOC with O₃ was similar for day and night
464 samples, which was 0.02 μg m⁻³ per ppbv ozone. For PKUERS, the increment rate of

465 the SOC towards ozone was $0.04 \mu\text{g m}^{-3}$ and $0.02 \mu\text{g m}^{-3}$ per ppbv ozone at day and
466 night, respectively.

467 **Influence of temperature and relative humidity on SOA formation**

468 Temperature was considered as a great influencing factor on SOA formation. On the
469 one hand, higher temperature promoted the evaporation of the semi volatile SOA. On
470 the other hand, high-temperature conditions would favor the oxidation, which would
471 accelerate the SOA formation (Saathoff et al., 2009). Fig. 4 (c) (d) showed the
472 variation of SOC concentrations with the temperature. In this study, SOC
473 concentration showed positive correlation with temperature at CP and PKUERS,
474 demonstrating that temperature favors the SOA formation in the summer of Beijing.
475 Moreover, different correlation of the day and the night samples imply the different
476 pathways of SOA formation. However, poor relations could be found between SOC
477 and RH.

478 **Effects of aqueous-phase acid catalyzed reactions on SOA formation**

479 Aerosol water and acidity have been considered to have great impact on the
480 aqueous-phase SOA formation (Cheng et al., 2016). To figure out the influences of
481 water content and aerosol acidity on the aqueous-phase reactions, ISORROPIA-II
482 thermodynamic equilibrium model was used (Surratt et al., 2007). The model was set
483 at forward mode, based on the concentrations of particle phase Na^+ , NH_4^+ , K^+ , Mg^{2+} ,
484 Ca^{2+} , NO_3^- , SO_4^{2-} , Cl^- and gaseous NH_3 as well as ambient temperature and RH.

485 Results showed that the average aerosol water content at CP was $3.87 \pm 3.73 \mu\text{g m}^{-3}$,
486 higher than that at PKUERS ($1.83 \pm 1.81 \mu\text{g m}^{-3}$). The water content was lower in
487 2016 than that in 2008. The estimated SOC concentration showed good correlations
488 with water content at both sites. Compared with CP, the correlation factor in PKUERS
489 was better, implying that aqueous phase reaction may be more important in the urban
490 area. Different correlation could be found at different liquid water contents, especially

491 for CP, where liquid water content spanned a wide range, implying that different
492 mechanisms may exist at different liquid water content.

493 In this study, modeled H^+ concentration and SOC showed significant correlation
494 ($p < 0.05$) at the two places, which indicated that acid-catalyzed reaction might provide
495 a crucial pathway for the SOA formation in the summer of Beijing. Laboratory studies
496 showed that acid-catalyzed reactive uptake might play great role in the enhancement
497 of SOA (Zhang et al., 2014; Surratt et al., 2010; Jang et al., 2002). However, contrary
498 conclusions were made by other group, demonstrating the inconsistency of the aerosol
499 acidity and the SOA formation (Wong et al., 2015; Kristensen et al., 2014). The
500 contradiction might give the facts that the impacts of the acidity on the SOA loading
501 varied from place to place, determined by the specific environmental conditions.
502 Linear regression showed that the enhancement of SOC with modeled H^+
503 concentration were at a value of $0.02 \mu\text{g m}^{-3}$ per nmol H^+ , which was lower than the
504 previous results (0.046 for PKUERS, and 0.041 for Yufa, 2008). Offenberg et al.
505 (Offenberg et al., 2009) discovered good correlation between SOC and $[H^+]_{\text{air}}$, with
506 R^2 value of 0.815. Besides, a one $\text{nmol m}^{-3} [H^+]_{\text{air}}$ would give rise to $0.015 \mu\text{g m}^{-3}$
507 SOC increase from the oxidation of α -pinene in the chamber experiment. **We also**
508 **analyzed the relationship between apportioned SOC and sulfate concentration and**
509 **found that the apportioned SOC increased with the increase of sulfate concentration.**
510 **The coefficient R^2 were 0.41 and 0.45 for CP and PKUERS, respectively, indicating**
511 **that the increase of SOC may be influenced by the sulfate aerosol. As such, the**
512 **increase in SOC is likely arise from the acid-catalyzed reactions with the participation**
513 **of sulfate aerosols.** In the present work, different correlations could be found at
514 different modeled H^+ concentrations where apportioned SOC increased significantly
515 as the H^+ concentration increased and then increased slowly at a certain level,
516 showing gradient growth at different hydrogen-ion concentrations. Therefore, aqueous
517 phase acid-catalyzed reactions may influence the SOA formation through different
518 mechanisms at varied level of liquid water concentration and aerosol acidity.

519 **5. Conclusion**

520 High concentrations of fine particles were observed during the “Campaign on
521 Photochemical Smog in China”, with the average mass concentrations of $45.48 \pm$
522 $19.78 \mu\text{g m}^{-3}$ and $42.99 \pm 17.50 \mu\text{g m}^{-3}$, at CP site and PKUERS site, respectively.
523 Compared with previous studies, the concentrations of $\text{PM}_{2.5}$, EC and estimated SOC
524 decreased significantly, due to the drastic measures implemented by the government
525 in the recent years. However, OC showed a higher concentration, suggesting
526 particulate organic matters become more and more important in Beijing. CMB
527 modeling and tracer-yield method were used to apportion the primary and secondary
528 organic aerosol sources. The apportioned primary and secondary OC accounted for
529 $62.8 \pm 18.3\%$ and $80.9 \pm 27.2\%$ of the measured OC at CP and PKUERS, respectively.
530 Vehicle emissions i.e. diesel and gasoline engine emissions were the major primary
531 organic aerosol sources, which contributed to $28.8 \pm 14.8\%$ and $37.6 \pm 19.3\%$ of the
532 OC at CP and PKUERS, respectively. Compared with the results of the previous work,
533 the gasoline engine emission contributed almost twice of that in 2008 (18.0% vs
534 10.0%), while the contribution of diesel engine emission decreased by 12.5%
535 compared with the result in 2008. Besides, the contributions of biomass burning and
536 coal combustion both decreased. The apportioned biogenic and anthropogenic SOC
537 can explain $20.2 \pm 6.7\%$ and $30.5 \pm 12.0\%$ of the measured OC at CP and PKUERS,
538 respectively. The contribution of toluene SOC is the highest among the apportioned
539 SOC, which is different from the results of the most developed countries in the world.
540 Our results revealed an important point, which is that controlling SOA seems feasible
541 in the developing countries like China. It is difficult to control SOA in developed
542 countries, since biogenic SOA are dominant. However, deducting anthropogenic
543 precursors may be an efficient way to reduce the SOA pollution where anthropogenic
544 SOA is dominant. Back trajectory clustering analysis showed that the particle source
545 contributions were similar when air masses were from different directions, suggesting
546 the regional organic particle pollution in Beijing. However, the higher organic particle

547 loading from south cluster indicates that there were more emissions from southern
548 region of Beijing. The present work also implied that the aqueous phase
549 acid-catalyzed reactions may be an important SOA formation mechanism in summer
550 of Beijing.

551 **Acknowledgement**

552 This research is supported by the National Key R&D Program of China
553 (2016YFC0202000, Task 3), the National Natural Science Foundation of China
554 (21677002), framework research program on ‘Photochemical smog in China’ financed
555 by Swedish Research Council (639-2013-6917).

556 **References**

- 557 Barmpadimos, I., Keller, J., Oderbolz, D., Hueglin, C., and Prévôt, A.: One decade of
558 parallel fine (PM_{2.5}) and coarse (PM₁₀–PM_{2.5}) particulate matter measurements in
559 Europe: trends and variability, *Atmos Chem Phys*, 12, 3189-3203, 2012.
- 560 Cao, J. J., Lee, S. C., Ho, K. F., Zou, S. C., Fung, K., Li, Y., Watson, J. G., and Chow,
561 J. C.: Spatial and seasonal variations of atmospheric organic carbon and
562 elemental carbon in Pearl River Delta Region, China, *Atmospheric Environment*,
563 38, 4444-4456, <http://doi.org/10.1016/j.atmosenv.2004.05.016>, 2004.
- 564 Cass, G. R.: Organic molecular tracers for particulate air pollution sources,
565 *Trac-Trends in Analytical Chemistry*, 17, 356-366,
566 10.1016/s0165-9936(98)00040-5, 1998.
- 567 Cheng, Y., Engling, G., He, K. B., and Duan, F. K.: Biomass burning contribution to
568 Beijing aerosol, *Atmospheric Chemistry & Physics*, 13, 7765-7781, 2013.
- 569 Cheng, Y., Zheng, G., Wei, C., Mu, Q., Zheng, B., Wang, Z., Gao, M., Zhang, Q., He,
570 K., and Carmichael, G.: Reactive nitrogen chemistry in aerosol water as a source
571 of sulfate during haze events in China, *Science Advances*, 2, e1601530, 2016.
- 572 Claeys, M., Graham, B., Vas, G., Wang, W., Vermeylen, R., Pashynska, V., Cafmeyer,
573 J., Guyon, P., Andreae, M. O., and Artaxo, P.: Formation of Secondary Organic
574 Aerosols Through Photooxidation of Isoprene, *Science*, 303, 1173, 2004.
- 575 Dan, M., Zhuang, G., Li, X., Tao, H., and Zhuang, Y.: The characteristics of
576 carbonaceous species and their sources in PM_{2.5} in Beijing, *Atmospheric
577 Environment*, 38, 3443-3452, <http://doi.org/10.1016/j.atmosenv.2004.02.052>,
578 2004.
- 579 Ding, X., Wang, X. M., Gao, B., Fu, X. X., He, Q. F., Zhao, X. Y., Yu, J. Z., and
580 Zheng, M.: Tracer - based estimation of secondary organic carbon in the Pearl
581 River Delta, south China, *Journal of Geophysical Research Atmospheres*, 117,
582 2012.

583 Ding, X., He, Q. F., Shen, R. Q., Yu, Q. Q., and Wang, X. M.: Spatial distributions of
584 secondary organic aerosols from isoprene, monoterpenes, beta-caryophyllene,
585 and aromatics over China during summer, *Journal of Geophysical*
586 *Research-Atmospheres*, 119, 11877-11891, 10.1002/2014jd021748, 2014.

587 El Haddad, I., Marchand, N., Temime-Roussel, B., Wortham, H., Piot, C., Besombes,
588 J. L., Baduel, C., Voisin, D., Armengaud, A., and Jaffrezo, J. L.: Insights into the
589 secondary fraction of the organic aerosol in a Mediterranean urban area:
590 Marseille, *Atmos Chem Phys*, 11, 2059-2079, 2011.

591 Fu, P., Aggarwal, S. G., Chen, J., Li, J., Sun, Y., Wang, Z., Chen, H., Liao, H., Ding,
592 A., Umarji, G. S., Patil, R. S., Chen, Q., and Kawamura, K.: Molecular Markers
593 of Secondary Organic Aerosol in Mumbai, India, *Environ. Sci. Technol.*, 50,
594 4659-4667, 10.1021/acs.est.6b00372, 2016.

595 Gao, J. J., Tian, H. Z., Cheng, K., Lu, L., Wang, Y. X., Wu, Y., Zhu, C. Y., Liu, K. Y.,
596 Zhou, J. R., Liu, X. G., Chen, J., and Hao, J. M.: Seasonal and spatial variation
597 of trace elements in multi-size airborne particulate matters of Beijing, China:
598 Mass concentration, enrichment characteristics, source apportionment, chemical
599 speciation and bioavailability, *Atmospheric Environment*, 99, 257-265,
600 10.1016/j.atmosenv.2014.08.081, 2014.

601 Ghirardo, A., J. Xie, X. Zheng, Y. Wang, R. Grote, K. Block, J. Wildt, T. Mentel, A.
602 Kiendler-Scharr, and M. Hallquist (2016), Urban stress-induced biogenic VOC
603 emissions and SOA-forming potentials in Beijing, *Atmospheric chemistry and*
604 *physics*, 16(5), 2901-2920.

605 Guo, S., Hu, M., Wang, Z. B., Slanina, J., and Zhao, Y. L.: Size-resolved aerosol
606 water-soluble ionic compositions in the summer of Beijing: implication of
607 regional secondary formation, *Atmos Chem Phys*, 10, 947-959, 2010.

608 Guo, S., Hu, M., Guo, Q., Zhang, X., Zheng, M., Zheng, J., Chang, C. C., Schauer, J.
609 J., and Zhang, R.: Primary Sources and Secondary Formation of Organic

610 Aerosols in Beijing, China, *Environmental Science & Technology*, 46,
611 9846-9853, 10.1021/es20425641, 2012.

612 Guo, S., Hu, M., Guo, Q., Zhang, X., Schauer, J., and Zhang, R.: Quantitative
613 evaluation of emission controls on primary and secondary organic aerosol
614 sources during Beijing 2008 Olympics, *Atmos Chem Phys*, 13, 8303-8314, 2013.

615 Guo, S., Hu, M., Zamora, M. L., Peng, J., Shang, D., Zheng, J., Du, Z., Wu, Z., Shao,
616 M., and Zeng, L.: Elucidating severe urban haze formation in China, *Proceedings*
617 *of the National Academy of Sciences*, 111, 17373-17378, 2014a.

618 Guo, S., Hu, M., Guo, Q. F., and Shang, D. J.: Comparison of Secondary Organic
619 Aerosol Estimation Methods, *Acta Chim Sinica*, 72, 658-666,
620 10.6023/A14040254, 2014b.

621 Guo, S., Hu, M., Shang, D., Guo, Q., and Hu, W.: Research on Secondary Organic
622 Aerosols Basing on Field Measurement, *Acta Chim. Sinica*, 72, 145-157, DOI:
623 10.6023/A13111169, 2014c.

624 Haque, M. M., Kawamura, K., and Kim, Y.: Seasonal variations of biogenic
625 secondary organic aerosol tracers in ambient aerosols from Alaska, *Atmospheric*
626 *Environment*, 130, 95-104, 10.1016/j.atmosenv.2015.09.075, 2016.

627 Hoyle, C., Boy, M., Donahue, N., Fry, J., Glasius, M., Guenther, A., Hallar, A., Huff
628 Hartz, K., Petters, M., and Petters, T.: A review of the anthropogenic influence on
629 biogenic secondary organic aerosol, *Atmospheric Chemistry and Physics*, 11,
630 321-343, 2011.

631 Hu, D., Bian, Q., Li, T. W., Lau, A. K., and Yu, J. Z.: Contributions of isoprene,
632 monoterpenes, β -caryophyllene, and toluene to secondary organic aerosols in
633 Hong Kong during the summer of 2006, *Journal of Geophysical Research:*
634 *Atmospheres*, 113, 2008.

635 Hu, D., Bian, Q., Lau, A. K. H., and Yu, J. Z.: Source apportioning of primary and
636 secondary organic carbon in summer PM_{2.5} in Hong Kong using positive matrix

637 factorization of secondary and primary organic tracer data, *Journal of*
638 *Geophysical Research Atmospheres*, 115, 2010

639 Hu, M., Guo, S., Peng, J.-f., and Wu, Z.-j.: Insight into characteristics and sources of
640 PM_{2.5} in the Beijing–Tianjin–Hebei region, China, *National Science Review*, 2,
641 257-258, 2015.

642 Huang, X.-F., He, L.-Y., Hu, M., and Zhang, Y.-H.: Annual variation of particulate
643 organic compounds in PM_{2.5} in the urban atmosphere of Beijing, *Atmospheric*
644 *Environment*, 40, 2449-2458, 2006.

645 Huang, X. F., He, L. Y., Hu, M., Canagaratna, M. R., Sun, Y., Zhang, Q., Zhu, T., Xue,
646 L., Zeng, L. W., and Liu, X. G.: Highly time-resolved chemical characterization
647 of atmospheric submicron particles during 2008 Beijing Olympic Games using
648 an Aerodyne High-Resolution Aerosol Mass Spectrometer, *Atmospheric*
649 *Chemistry & Physics Discussions*, 10, 8933-8945, 2010.

650 Jang, M. S., Czoschke, N. M., Lee, S., and Kamens, R. M.: Heterogeneous
651 atmospheric aerosol production by acid-catalyzed particle-phase reactions,
652 *Science*, 298, 814-817, 10.1126/science.1075798, 2002.

653 Kleindienst, T. E., Jaoui, M., Lewandowski, M., Offenberg, J. H., Lewis, C. W.,
654 Bhave, P. V., and Edney, E. O.: Estimates of the contributions of biogenic and
655 anthropogenic hydrocarbons to secondary organic aerosol at a southeastern US
656 location, *Atmospheric Environment*, 41, 8288-8300, 2007.

657 Kleindienst, T., Michael Lewandowski, Offenberg, J., Edney, E., Mohammed Jaoui,
658 Mei Zheng, Xiang Ding, and Edgerton, E.: Contribution of Primary and
659 Secondary Sources to Organic Aerosol and PM_{2.5} at SEARCH Network Sites,
660 *Journal of the Air & Waste Management Association*, 60, 1388, 2010.

661 Kourtchev, I., Warnke, J., Maenhaut, W., Hoffmann, T., and Claeys, M.: Polar organic
662 marker compounds in PM_{2.5} aerosol from a mixed forest site in western
663 Germany, *Chemosphere*, 73, 1308-1314, 2008.

664 Kristensen, K., Cui, T., Zhang, H., Gold, A., Glasius, M., and Surratt, J.: Dimers in
665 α -pinene secondary organic aerosol: effect of hydroxyl radical, ozone, relative
666 humidity and aerosol acidity, *Atmos Chem Phys*, 14, 4201-4218, 2014.

667 Lambe, A. T., Miracolo, M. A., Hennigan, C. J., Robinson, A. L., and Donahue, N. M.:
668 Effective Rate Constants and Uptake Coefficients for the Reactions of Organic
669 Molecular Markers (n-Alkanes, Hopanes, and Steranes) in Motor Oil and Diesel
670 Primary Organic Aerosols with Hydroxyl Radicals, *Environ. Sci. Technol.*, 43,
671 8794-8800, 10.1021/es901745h, 2009.

672 Lappalainen, H., Sevanto, S., Bäck, J., Ruuskanen, T., Kolari, P., Taipale, R., Rinne, J.,
673 Kulmala, M., and Hari, P.: Day-time concentrations of biogenic volatile organic
674 compounds in a boreal forest canopy and their relation to environmental and
675 biological factors, *Atmospheric Chemistry and Physics*, 9, 5447-5459, 2009.

676 Lewandowski, M., Jaoui, M., Offenberg, J. H., Kleindienst, T. E., Edney, E. O.,
677 Sheesley, R. J., and Schauer, J. J.: Primary and secondary contributions to
678 ambient PM in the midwestern United States, *Environmental Science &
679 Technology*, 42, 3303-3309, 2008.

680 Liu, Q. Y., Baumgartner, J., Zhang, Y., and Schauer, J. J.: Source apportionment of
681 Beijing air pollution during a severe winter haze event and associated
682 pro-inflammatory responses in lung epithelial cells, *Atmospheric Environment*,
683 126, 28-35, 10.1016/j.atmosenv.2015.11.031, 2016.

684 Lough, G. C., Christensen, C. G., Schauer, J. J., Tortorelli, J., Mani, E., Lawson, D. R.,
685 Clark, N. N., and Gabele, P. A.: Development of molecular marker source
686 profiles for emissions from on-road gasoline and diesel vehicle fleets, *J. Air
687 Waste Manage. Assoc.*, 57, 1190-1199, 10.3155/1047-3289.57.10.1190, 2007.

688 Hallquist, M., Munthe, J., Hu, M., Wang, T., Chan, C. K., Gao, J., Boman, J., Guo, S.,
689 Hallquist, Å. M., and Mellqvist, J.: Photochemical smog in China: scientific
690 challenges and implications for air-quality policies, *National Science Review*, 3,
691 401-403, 2016.

692 Miyazaki, Y., Jung, J., Fu, P., Mizoguchi, Y., Yamanoi, K., and Kawamura, K.:
693 Evidence of formation of submicrometer water - soluble organic aerosols at a
694 deciduous forest site in northern Japan in summer, *Journal of Geophysical*
695 *Research: Atmospheres*, 117, 2012.

696 Offenberg, J. H., Lewis, C. W., Lewandowski, M., Jaoui, M., Kleindienst, T. E., and
697 Edney, E. O.: Contributions of toluene and alpha-pinene to SOA formed in an
698 irradiated toluene/alpha-pinene/NO(x)/ air mixture: comparison of results using
699 ¹⁴C content and SOA organic tracer methods, *Environmental Science &*
700 *Technology*, 41, 3972-3976, 2007.

701 Offenberg, J. H., Lewandowski, M., Edney, E. O., Kleindienst, T. E., and Jaoui, M.:
702 Influence of Aerosol Acidity on the Formation of Secondary Organic Aerosol
703 from Biogenic Precursor Hydrocarbons, *Environ. Sci. Technol.*, 43, 7742-7747,
704 10.1021/es901538e, 2009.

705 Oros, D. R., and Simoneit, B. R. T.: Identification and emission rates of molecular
706 tracers in coal smoke particulate matter, *Fuel*, 79, 515-536, Doi
707 10.1016/S0016-2361(99)00153-2, 2000.

708 Park, S. S., and Cho, S. Y.: Tracking sources and behaviors of water-soluble organic
709 carbon in fine particulate matter measured at an urban site in Korea, *Atmospheric*
710 *environment*, 45, 60-72, 2011.

711 Rogge, W. F., Hildemann, L. M., Mazurek, M. A., Cass, G. R., and Simoneit, B. R. T.:
712 Sources of fine organic aerosol. 4. Particulate abrasion products from leaf
713 surfaces of urban plants, *Environ. Sci. Technol.*, 27, 2700-2711, 1993.

714 Saathoff, H., Naumann, K.-H., Möhler, O., Jonsson, Å. M., Hallquist, M.,
715 Kiendler-Scharr, A., Mentel, T. F., Tillmann, R., and Schurath, U.: Temperature
716 dependence of yields of secondary organic aerosols from the ozonolysis of
717 α -pinene and limonene, *Atmos Chem Phys*, 9, 1551-1577, 2009.

718 Schauer, J. J., Rogge, W. F., Hildemann, L. M., Mazurek, M. A., Cass, G. R., and
719 Simoneit, B. R. T.: Source apportionment of airborne particulate matter using

720 organic compounds as tracers, *Atmospheric Environment*, 30, 3837-3855,
721 10.1016/1352-2310(96)00085-4, 1996.

722 Sheesley, R. J., Schauer, J. J., Zheng, M., and Wang, B.: Sensitivity of molecular
723 marker-based CMB models to biomass burning source profiles, *Atmospheric*
724 *Environment*, 41, 9050-9063, 2007.

725 Simoneit, B. R., Schauer, J. J., Nolte, C., Oros, D. R., Elias, V. O., Fraser, M., Rogge,
726 W., and Cass, G. R.: Levoglucosan, a tracer for cellulose in biomass burning and
727 atmospheric particles, *Atmospheric Environment*, 33, 173-182, 1999.

728 Song, G., Min, H., Qingfeng, G., and Dongjie, S.: Comparison of secondary organic
729 aerosol estimation methods, *ACTA CHIMICA SINICA*, 72, 658-666, 2014.

730 Song, Y., Zhang, Y., Xie, S., Zeng, L., Zheng, M., Salmon, L. G., Shao, M., and
731 Slanina, S.: Source apportionment of PM_{2.5} in Beijing by positive matrix
732 factorization, *Atmospheric Environment*, 40, 1526-1537, 2006.

733 Stone, E. A., Nguyen, T. T., Pradhan, B. B., and Dangol, P. M.: Assessment of
734 biogenic secondary organic aerosol in the Himalayas, *Environmental Chemistry*,
735 9, 263-272, 2012.

736 Sun, J., Zhang, Q., Canagaratna, M. R., Zhang, Y., Ng, N. L., Sun, Y., Jayne, J. T.,
737 Zhang, X., Zhang, X., and Worsnop, D. R.: Highly time- and size-resolved
738 characterization of submicron aerosol particles in Beijing using an Aerodyne
739 Aerosol Mass Spectrometer, *Atmospheric Environment*, 44, 131-140, 2010.

740 Surratt, J. D., Kroll, J. H., Kleindienst, T. E., Edney, E. O., Claeys, M., Sorooshian, A.,
741 Ng, N. L., Offenberg, J. H., Lewandowski, M., Jaoui, M., Flagan, R. C., and
742 Seinfeld, J. H.: Evidence for organosulfates in secondary organic aerosol,
743 *Environ. Sci. Technol.*, 41, 517-527, 10.1021/es062081q, 2007.

744 Surratt, J. D., Chan, A. W., Eddingsaas, N. C., Chan, M., Loza, C. L., Kwan, A. J.,
745 Hersey, S. P., Flagan, R. C., Wennberg, P. O., and Seinfeld, J. H.: Reactive
746 intermediates revealed in secondary organic aerosol formation from isoprene,
747 *Proceedings of the National Academy of Sciences*, 107, 6640-6645, 2010.

748 Tai, A. P., Mickley, L. J., and Jacob, D. J.: Correlations between fine particulate matter
749 (PM 2.5) and meteorological variables in the United States: Implications for the
750 sensitivity of PM 2.5 to climate change, *Atmospheric Environment*, 44,
751 3976-3984, 2010.

752 Tan, J. H., Duan, J. C., Chai, F. H., He, K. B., and Hao, J. M.: Source apportionment
753 of size segregated fine/ultrafine particle by PMF in Beijing, *Atmospheric
754 Research*, 139, 90-100, 10.1016/j.atmosres.2014.01.007, 2014.

755 Tao, J., Zhang, L., Cao, J., Zhong, L., Chen, D., Yang, Y., Chen, D., Chen, L., Zhang,
756 Z., Wu, Y., Xia, Y., Ye, S., and Zhang, R.: Source apportionment of PM2.5 at
757 urban and suburban areas of the Pearl River Delta region, south China - With
758 emphasis on ship emissions, *Science of the Total Environment*, 574, 1559-1570,
759 10.1016/j.scitotenv.2016.08.175, 2017.

760 Tian, S. L., Pan, Y. P., and Wang, Y. S.: Size-resolved source apportionment of
761 particulate matter in urban Beijing during haze and non-haze episodes, *Atmos
762 Chem Phys*, 16, 1-19, 10.5194/acp-16-1-2016, 2016.

763 Turpin, B. J., and Huntzicker, J. J.: Identification of secondary organic aerosol
764 episodes and quantitation of primary and secondary organic aerosol
765 concentrations during SCAQS, *Atmospheric Environment*, 29, 3527-3544, 1995.

766 Wang, B., Shao, M., Lu, S., Yuan, B., Zhao, Y., Wang, M., Zhang, S., and Wu, D.:
767 Variation of ambient non-methane hydrocarbons in Beijing city in summer 2008,
768 *Atmospheric Chemistry and Physics*, 10, 5911, 2010.

769 Wang, Q., Shao, M., Zhang, Y., Wei, Y., Hu, M., and Guo, S.: Source apportionment
770 of fine organic aerosols in Beijing, *Atmospheric Chemistry and Physics*, 9,
771 8573-8585, 2009.

772 Wang, X., Bi, X., Sheng, G., and Fu, J.: Chemical composition and sources of PM10
773 and PM2. 5 aerosols in Guangzhou, China, *Environmental Monitoring and
774 Assessment*, 119, 425-439, 2006.

775 Wong, J. P. S., Lee, A. K. Y., and Abbatt, J. P. D.: Impacts of Sulfate Seed Acidity and
776 Water Content on Isoprene Secondary Organic Aerosol Formation, *Environ. Sci.*
777 *Technol.*, 49, 13215-13221, 10.1021/acs.est.5b02686, 2015.

778 Wu, Y., Guo, J., Zhang, X., and Li, X.: Correlation between PM concentrations and
779 Aerosol Optical Depth in eastern China based on BP neural networks,
780 *Geoscience and Remote Sensing Symposium*, 2011, 5876-5886.

781 Xiang, P., Zhou, X. M., Duan, J. C., Tan, J. H., He, K. B., Yuan, C., Ma, Y. L., and
782 Zhang, Y. X.: Chemical characteristics of water-soluble organic compounds
783 (WSOC) in PM_{2.5} in Beijing, China: 2011-2012, *Atmos. Res.*, 183, 104-112,
784 10.1016/j.atmosres.2016.08.020, 2017.

785 Yang, F., Kawamura, K., Chen, J., Ho, K. F., Lee, S. C., Gao, Y., Cui, L., Wang, T. G.,
786 and Fu, P. Q.: Anthropogenic and biogenic organic compounds in summertime
787 fine aerosols (PM_{2.5}) in Beijing, China, *Atmospheric Environment*, 124,
788 166-175, 10.1016/j.atmosenv.2015.08.095, 2016.

789 Yttri, K. E., Simpson, D., Nojgaard, J. K., Kristensen, K., Genberg, J., Stenstrom, K.,
790 Swietlicki, E., Hillamo, R., Aurela, M., Bauer, H., Offenberg, J. H., Jaoui, M.,
791 Dye, C., Eckhardt, S., Burkhardt, J. F., Stohl, A., and Glasius, M.: Source
792 apportionment of the summer time carbonaceous aerosol at Nordic rural
793 background sites, *Atmos Chem Phys*, 11, 13339-13357, 2011.

794 Yu, L. D., Wang, G. F., Zhang, R. J., Zhang, L. M., Song, Y., Wu, B. B., Li, X. F., An,
795 K., and Chu, J. H.: Characterization and Source Apportionment of PM_{2.5} in an
796 Urban Environment in Beijing, *Aerosol Air Qual Res*, 13, 574-583,
797 10.4209/aaqr.2012.07.0192, 2013.

798 Zhang, H., Zhang, Z., Cui, T., Lin, Y.-H., Bhathela, N. A., Ortega, J., Worton, D. R.,
799 Goldstein, A. H., Guenther, A., Jimenez, J. L., Gold, A., and Surratt, J. D.:
800 Secondary Organic Aerosol Formation via 2-Methyl-3-buten-2-ol Photooxidation:
801 Evidence of Acid-Catalyzed Reactive Uptake of Epoxides, *Environmental*
802 *Science & Technology Letters*, 1, 242-247, 10.1021/ez500055f, 2014.

803 Zhang, Q., Streets, D. G., Carmichael, G. R., He, K. B., Huo, H., Kannari, A.,
804 Klimont, Z., Park, I. S., Reddy, S., Fu, J. S., Chen, D., Duan, L., Lei, Y., Wang, L.
805 T., and Yao, Z. L.: Asian emissions in 2006 for the NASA INTEX-B mission,
806 *Atmos Chem Phys*, 9, 5131-5153, 2009.

807 Zhang, R., Jing, J., Tao, J., Hsu, S.-C., Wang, G., Cao, J., Lee, C. S. L., Zhu, L., Chen,
808 Z., and Zhao, Y.: Chemical characterization and source apportionment of PM 2.5
809 in Beijing: seasonal perspective, *Atmos Chem Phys*, 13, 7053-7074, 2013.

810 Zhang, Y. X., Sheesley, R. J., Schauer, J. J., Lewandowski, M., Jaoui, M., Offenberg, J.
811 H., Kleindienst, T. E., and Edney, E. O.: Source apportionment of primary and
812 secondary organic aerosols using positive matrix factorization (PMF) of
813 molecular markers, *Atmospheric Environment*, 43, 5567-5574, 2009.

814 Zhang, Y., Cai, J., Wang, S., He, K., and Zheng, M.: Review of receptor-based source
815 apportionment research of fine particulate matter and its challenges in China,
816 *The Science of the total environment*, 586, 917-929,
817 10.1016/j.scitotenv.2017.02.071, 2017.

818 Zheng, J., Hu, M., Peng, J., Wu, Z., Kumar, P., Li, M., Wang, Y., and Guo, S.: Spatial
819 distributions and chemical properties of PM 2.5 based on 21 field campaigns at
820 17 sites in China, *Chemosphere*, 159, 480-487, 2016a.

821 Zheng, M., Salmon, L. G., Schauer, J. J., Zeng, L., Kiang, C., Zhang, Y., and Cass, G.
822 R.: Seasonal trends in PM2. 5 source contributions in Beijing, China,
823 *Atmospheric Environment*, 39, 3967-3976, 2005.

824 Zheng, X. X., Guo, X. Y., Zhao, W. J., Shu, T. T., Xin, Y. A., Yan, X., Xiong, Q. L.,
825 Chen, F. T., and Lv, M.: Spatial variation and provenance of atmospheric trace
826 elemental deposition in Beijing, *Atmos. Pollut. Res.*, 7, 260-267,
827 10.1016/j.apr.2015.10.006, 2016b.

828 Zhou, J. B., Xiong, Y., Xing, Z. Y., Deng, J. J., and Du, K.: Characterizing and
829 sourcing ambient PM2.5 over key emission regions in China II: Organic

830 molecular markers and CMB modeling, *Atmospheric Environment*, 163, 57-64,
831 10.1016/j.atmosenv.2017.05.033, 2017.

832 Zhu, C., Kawamura, K., and Fu, P.: Seasonal variations of biogenic secondary organic
833 aerosol tracers in Cape Hedo, Okinawa, *Atmospheric Environment*, 130, 113-119,
834 10.1016/j.atmosenv.2015.08.069, 2016.

835 Zhu, Y., Yang, L., Kawamura, K., Chen, J., Ono, K., Wang, X., Xue, L., and Wang, W.:
836 Contributions and source identification of biogenic and anthropogenic
837 hydrocarbons to secondary organic aerosols at Mt. Tai in 2014, *Environmental*
838 *Pollution*, 220, 863-872, 10.1016/j.envpol.2016.10.070, 2017.

Table

Table 1. Summer PM_{2.5} mass concentrations in Beijing from 2008-2016, average \pm standard deviation ($\mu\text{g m}^{-3}$).

Year/Month	2008/07	2009/07	2010/05	2016/05-06	2016/05-06
Site	PKUERS	PKUERS	PKUERS	CP	PKUERS
	($\mu\text{g m}^{-3}$)				
PM _{2.5}	92.3 \pm 44.7	88.2 \pm 52.3	62.7 \pm 36.5	43.0 \pm 17.5	45.5 \pm 19.8
OC	10.4 \pm 2.9	8.5 \pm 2.5	8.9 \pm 4.5	8.9 \pm 3.2	11.0 \pm 3.7
EC	3.3 \pm 1.5	2.5 \pm 0.9	2.1 \pm 1.1	0.7 \pm 0.5	1.8 \pm 1.0
SO ₄ ²⁻	35.6 \pm 24.7	25.5 \pm 18.6	11.8 \pm 9.8	7.9 \pm 5.7	4.7 \pm 3.4
NO ₃ ⁻	7.9 \pm 6.9	17.8 \pm 13.2	10.0 \pm 11.2	3.4 \pm 3.3	2.4 \pm 2.3
NH ₄ ⁺	15.2 \pm 11.3	13.5 \pm 8.4	5.9 \pm 5.9	4.6 \pm 3.0	3.5 \pm 3.5
Ref.	(Guo et al., 2012)	(Zheng et al., 2016a)	(Zheng et al., 2016a)	This study	This study

Figure captions

Fig. 1 Concentrations of organic carbon from primary and secondary organic sources at (a) CP and (b) PKUERS as well as their contributions to the measured organic carbon at (c) CP and (d) PKUERS (%).

Fig. 2 Comparison of the sources at PKUERS between 2016 and 2008

Fig. 3 Particle sources from different air mass origins

Fig. 4 Correlations between SOC and different influencing factors (a)-(b) ozone, (c)-(d) temperature, (e)-(f) water and (g)-(h) H^+ concentratio

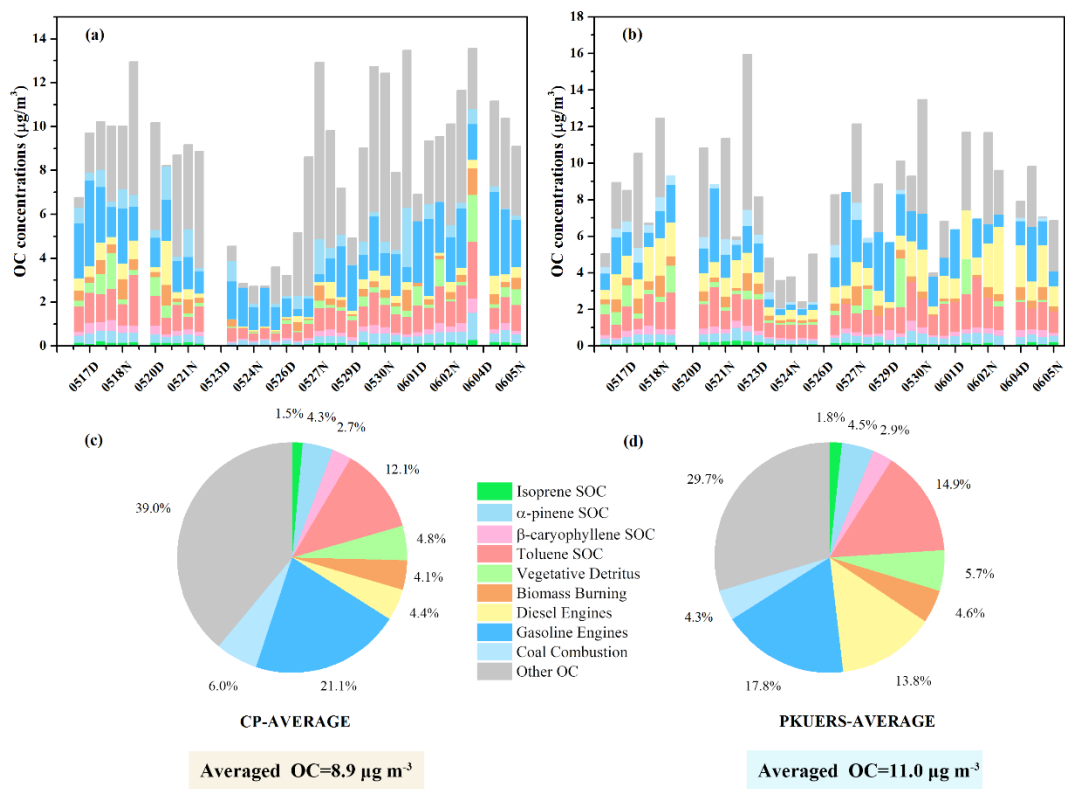


Fig. 1 Concentrations of organic carbon from primary and secondary organic sources at (a) CP and (b) PKUERS as well as their contributions to the measured organic carbon at (c) CP and (d) PKUERS (%).

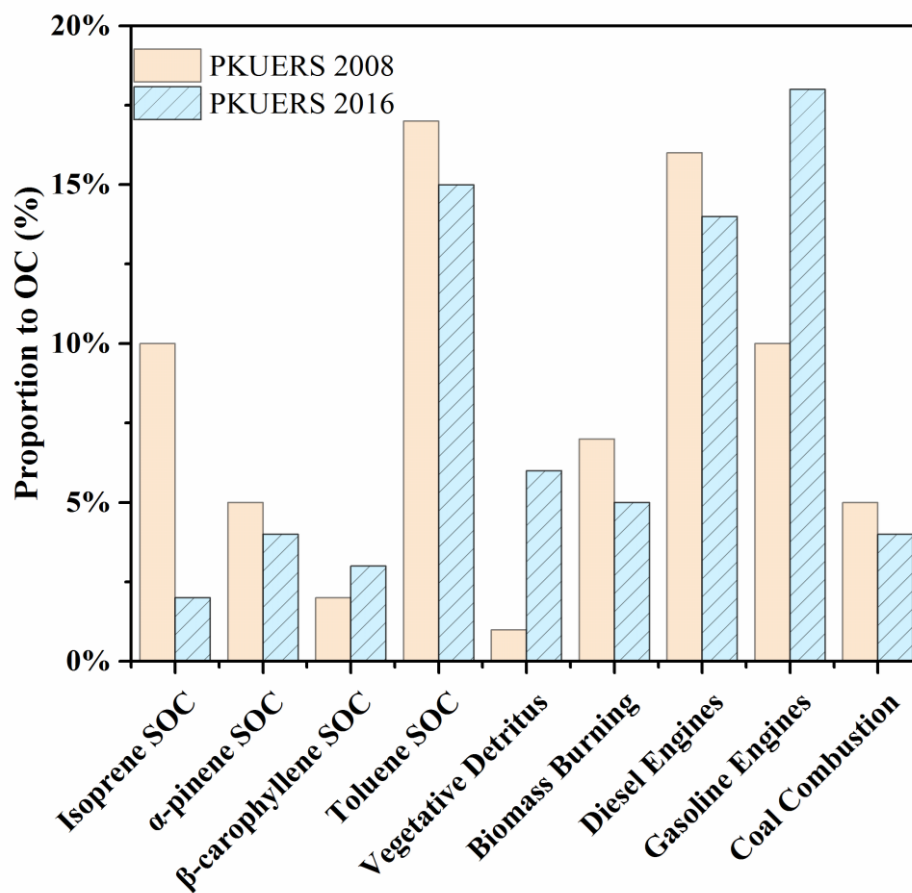


Fig.2 Comparison of the sources at PKUERS between 2016 and 2008 (Guo et al. 2012)

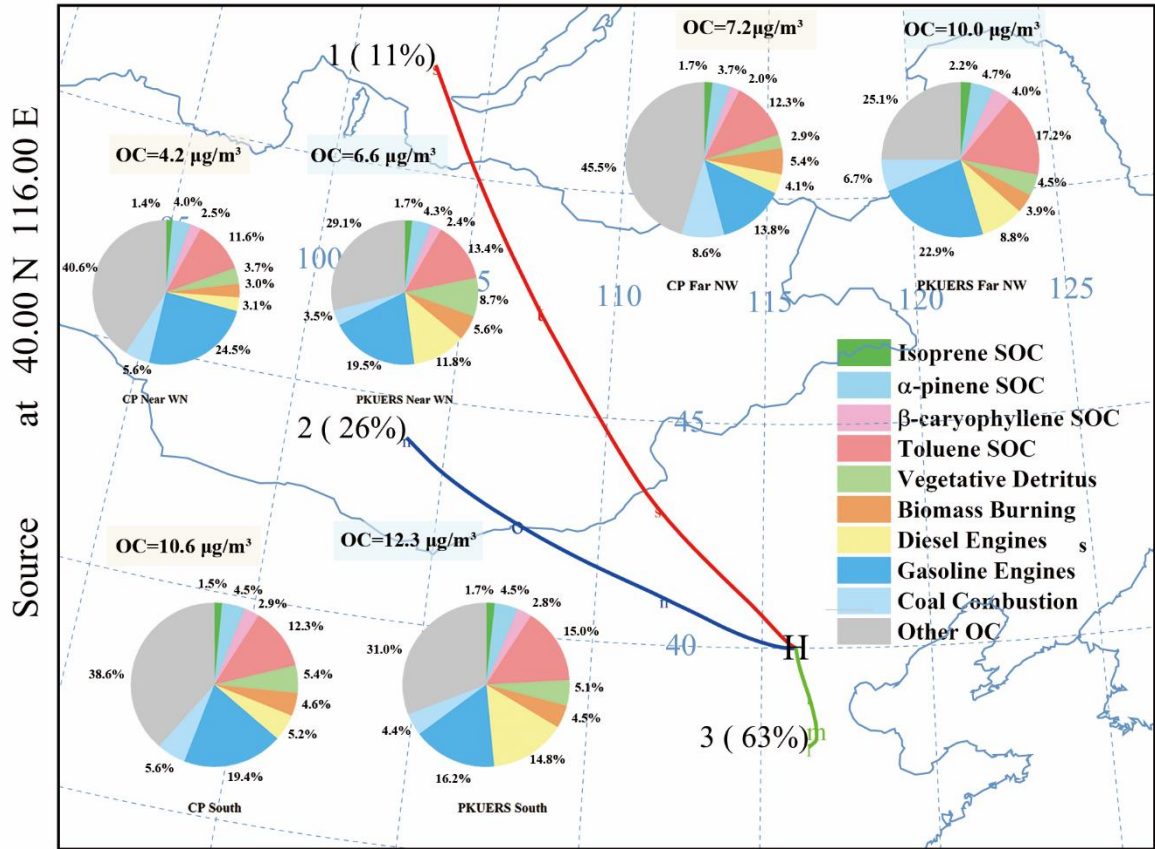


Fig. 3 Particle sources from different air mass origins

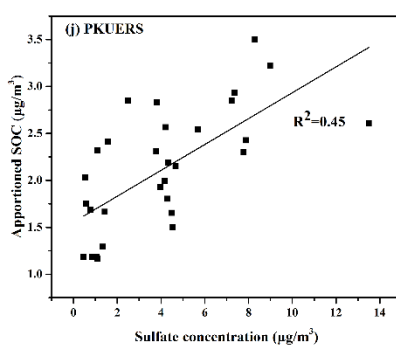
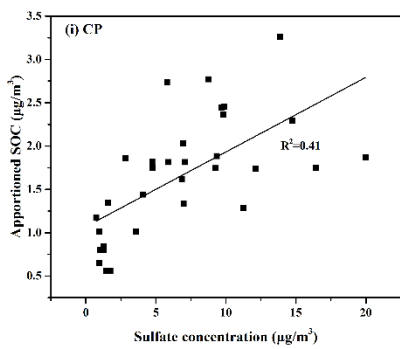
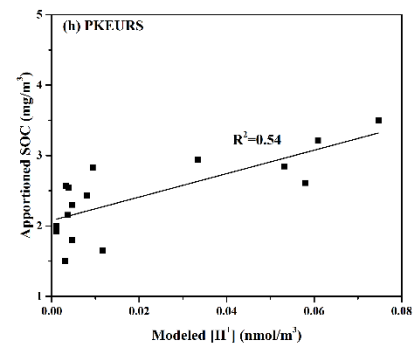
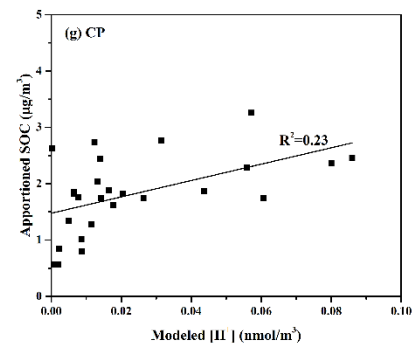
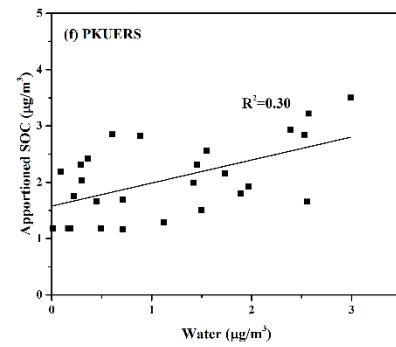
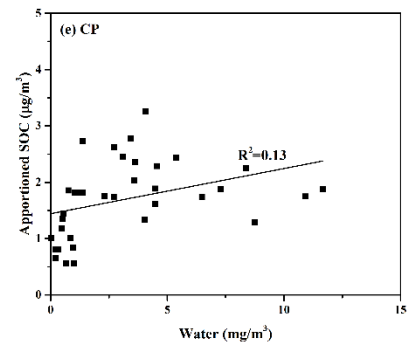
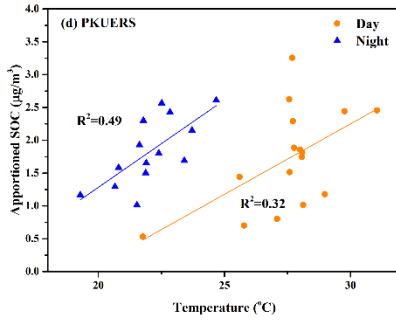
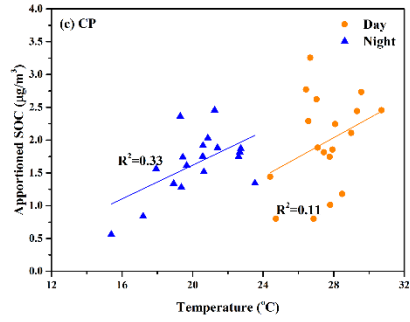
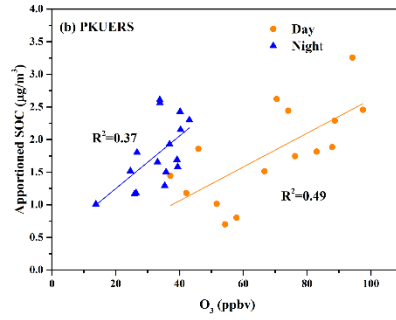
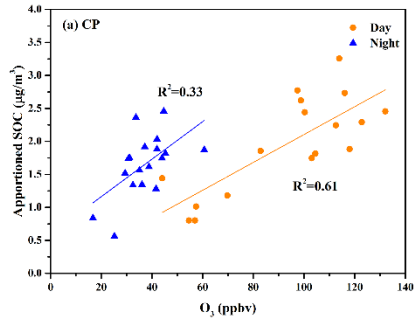


Fig. 4 Correlations between SOC and different influencing factors (a)-(b) ozone, (c)-(d) temperature, (e)-(f) water and (g)-(h) H⁺ concentration (i)-(j) sulfate concentration